

## Environmental Application of the BaPb<sub>0.9</sub>Sb<sub>0.1</sub>O<sub>3</sub> Perovskite: Guaiacol Electrodegradation

A. Rodrigues, J. Pereira, L. Ciríaco, A. Lopes, M. J. Pacheco\*

*FibEnTech/MTP and Department of Chemistry, University of Beira Interior,  
6201-001 Covilhã, Portugal*

Received 28 May 2014; accepted 28 June 2014

---

### Abstract

The perovskite BaPb<sub>0.9</sub>Sb<sub>0.1</sub>O<sub>3</sub> was prepared through the ceramic route and, after being chemical, structural and electrochemically characterized, it was used in the electrochemical oxidation of guaiacol, using Na<sub>2</sub>SO<sub>4</sub> as electrolyte, at current densities of 5 and 10 mA cm<sup>-2</sup> and initial guaiacol concentrations of 50, 100 and 200 mg L<sup>-1</sup>. The guaiacol degradation was followed by UV-Visible absorbance measurements, Chemical Oxygen Demand (COD) tests and Dissolved Organic Carbon (DOC) analysis. The combustion efficiency was also determined. Results have shown COD removals between 40 and 85 % and DOC removals from 34 to 66 % after 120 h assays. The absolute COD and DOC removals increase with guaiacol initial concentration and applied current density. The mineralization tendency, measured as the combustion efficiency, was maximum for the applied current density of 10 mA cm<sup>-2</sup> and a guaiacol initial concentration of 200 mg L<sup>-1</sup>.

**Keywords:** Electrochemical degradation; Guaiacol; Perovskite; BaPb<sub>0.9</sub>Sb<sub>0.1</sub>O<sub>3</sub>.

---

### Introduction

The denomination perovskite was first given to calcium titanium oxide mineral species with the chemical formula CaTiO<sub>3</sub>. Nowadays, it is considered perovskite any material that adopts the same structure as CaTiO<sub>3</sub>, with the general formula ABX<sub>3</sub>, where A is a large cation, which can be a rare earth, an alkaline or alkaline-earth metal, B a smaller cation, usually a transition metal, and X is a chalcogen or a halogen anion.

Metallic oxides that present perovskite like structure ABO<sub>3</sub> are very promising in terms of technological applications, namely as electrode materials [1,2]. In the

---

\* Corresponding author. E-mail address: mjap@ubi.pt

last years, many of these oxides have been used in solid fuel cells applications, as anodes, cathodes or even as solid electrolyte [3,4]. Several perovskites were also applied as electrode materials for electrocatalysis in the anodic evolution of  $O_2$  and  $Cl_2$ , since they have high electrochemical stability in basic solutions and suitable electrical conductivity [5-7]. These characteristics can make them also potentially good anode materials to be used in the oxidation of organic compounds [8-10].

Perovskite oxides can allow significant partial substitution of the B cation by a similar one, as in the case of the  $BaPb_{1-x}Sb_xO_3$  family, that presents solubility up to  $x \leq 0.3$  [10-12]. From this perovskite family, the  $BaPb_{0.9}Sb_{0.1}O_3$  was already used as anode in the electrodegradation of three azo dyes [8]. In this study, almost total color removal was attained and the highest chemical oxygen demand (COD) and total organic carbon removals obtained were 70 and 40%, respectively. In a recent publication,  $BaPb_{1-x}Sb_xO_3$  electrodes were prepared for  $x=0.0, 0.1, 0.2$  and  $0.3$  and used as anode material in the electrochemical degradation of the tetra-azo dye Direct Red 80 [10]. All the oxides lead to complete color removal, but the highest COD removal was obtained with the  $BaPbO_3$ . However, in order to reduce energetic costs it is crucial that the anode material presents suitable conductivity, and, according to Yasukawa et al. [12], in the  $BaPb_{1-x}Sb_xO_3$  perovskite family with different Pb/Sb ratios the perovskite  $BaPb_{0.9}Sb_{0.1}O_3$  is the oxide that presents higher conductivity. Thus, in this work, this perovskite was chosen to be used as anode material for the degradation of an organic pollutant, the guaiacol, to evaluate the potential application of this electrode material in the electrochemical treatment of lignin derived compounds rejected in the effluents of pulp and paper industries.

Guaiacol is a phenolic natural lignin product, first isolated from Guaiac resin. Among the harmful organic compounds, the phenolic compounds have deserved a special attention because of their toxicity and the frequency that they appear in industrial wastewaters, namely in the pulp and paper industries [13,14]. The one-electron oxidation product of guaiacol is a dimmer that absorbs at 470 nm [15]. In the presence of an excess of dimmers, guaiacol can undergo polymerisation, making its degradation more difficult.

Guaiacol electrodegradation was already performed by anodic oxidation, with very good results, using as anode a boron-doped diamond electrode [16]. A similar compound, 4-chloro-guaiacol, was also the target of a successful electrochemical degradation study, using as anode material  $PbO_2$  [17]. In fact, electrochemical methods offer a promising alternative as tertiary treatments to complement biological processes, with the advantage of being environmental compatible, due to the fact that the main reagent is the electron [18, 19]. These methods, when properly scaled, allow the conversion of organic compounds into less toxic substances or their complete mineralization. Due to this, electrochemical oxidation of aqueous solutions containing non-biodegradable phenolic compounds has been extensively studied [16, 20-25].

## Experimental

### *Electrodes preparation*

The BaPb<sub>0.9</sub>Sb<sub>0.1</sub>O<sub>3</sub> powder samples were prepared by conventional solid-state reaction [12]. Stoichiometric amounts of BaCO<sub>3</sub> (Merck, +99%), PbO<sub>2</sub> (Riedel-Haen, +99%) and Sb<sub>2</sub>O<sub>3</sub> (Merck, +99%) were mixed and grounded in an agate mortar and heated at 1123 K, in a tubular furnace (Carbolite, model STF 16/75, equipped with a temperature controller Eurotherm 808), for 48 h; intermediate regrinding and posterior heating for 12 h was carried out. The samples crystallographic structures were characterized by X-ray powder diffraction (XRD). The XRD patterns were collected on a Rigaku, model DMAX III/C with automatic data acquisition (APD Philips v3.5B), equipped with a monochromatized Cu K $\alpha$  radiation ( $\lambda$ = 0.15406 nm), operating at 40 mA and 30 kV. The recording conditions were 2 $\theta$  between 10 and 90° at a scanning rate of 1.2 °/min.

The powders morphological characterization was done by scanning electron microscopy (SEM) using a Hitachi, model S2700, operating at 20 keV. The samples were previously coated with gold.

The perovskite disc electrodes were prepared by pressing the powders into 1.3 cm<sup>2</sup> geometric area pellets, which were sintered at the synthesis temperature, for 12 hours. The ohmic contacts were done gluing a silver disc (with a welded copper wire) to the pellet with a silver epoxy resin. This device was mounted at the bottom of a cylindrical glass tube and sealed with epoxy resin, thus avoiding any contact between the solution and the silver disc or the copper wire.

### *Cyclic voltammetry measurements*

Cyclic voltammetry (CV) studies were carried out in a three electrodes cell with an Ag/AgCl, KCl<sub>sat</sub> reference electrode, a Pt wire counter electrode and a perovskite pellet working electrode. Solutions of 5 g L<sup>-1</sup> Na<sub>2</sub>SO<sub>4</sub> were used, in the absence and in the presence of different guaiacol contents, and were deaerated with bubbling N<sub>2</sub>. The cell was connected to a potentiostat/galvanostat Voltalab, 40 model PGZ301. The voltammograms were recorded in the potential region from -0.5 to 2.5 V, at a potential sweep rate of 20 mV s<sup>-1</sup>.

### *Electrodegradation experiments*

The electrochemical treatments were performed in a one-compartment cell using a power supply (GW Lab DC, model: GPS-3030D). The perovskite electrode disc was used as anode and a platinum foil, with 2 cm<sup>2</sup> geometric area, as cathode. Four different electrodes were used randomly in the assays that were run in triplicate. All anodic oxidations assays were performed in galvanostatic conditions, with applied current densities of 5 and 10 mA cm<sup>-2</sup> and the treatment duration was 120 hours. The guaiacol (Aldrich, +98 %) concentrations studied were 50, 100 and 200 mg L<sup>-1</sup>. As the paper industry effluents usually present high sulphate content, sodium sulphate (Merck, +99 %) with a concentration of 5 g L<sup>-1</sup> was chosen as electrolyte.

The electrodegradation assays were monitored by UV-visible absorption spectrophotometry, using a Shimadzu UV-1800 spectrophotometer. The trend of

the oxidation was monitored by COD determinations using the closed reflux titrimetric method, according to standard procedures [26] and, in order to follow the mineralization index of organic compounds, the Dissolved Organic Carbon (DOC) content was also measured using a Shimadzu TOC analyzer, model TOC-VCPH.

## Results and discussion

### *Structural and morphological characterization of the powder samples and electrodes*

Fig. 1 presents the diffraction patterns obtained for the  $\text{BaPb}_{0.9}\text{Sb}_{0.1}\text{O}_3$  powder samples. Considering  $\text{BaPbO}_3$  patterns, no extra diffraction lines were observed for the  $\text{BaPb}_{0.9}\text{Sb}_{0.1}\text{O}_3$  sample, indicating the presence of a single phase material, as expected due to the solubility of Sb in this perovskite family (up to  $x=0.3$ ) [10,12]. Using the programme UnitCell [27], it was concluded that the substitution of 10% of Pb by Sb does not change the cell parameter, which remains  $a=0.4265$  nm, like  $\text{BaPbO}_3$ .

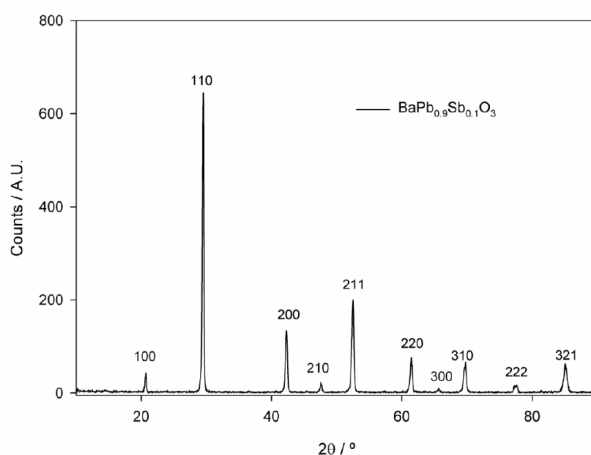


**Figure 1.** X-ray diffraction patterns of  $\text{BaPb}_{0.9}\text{Sb}_{0.1}\text{O}_3$  powder samples.

Electrodes morphological characterization shows a homogeneous surface with the crystallite dimensions of approximately  $0.3 \mu\text{m}$  (Fig. 2, a and b). The morphological characterization of the electrodes surface was also performed after having been used in the electrodegradation assays (Figure 2, c). Although the surface of the used material still presents a compact look, without evidence of disaggregation, a smoothness in the surface can be observed, probably due to some abrasion. However, the material in the interior of the electrode pellet still keeps the morphological characteristics of the original material (Figure 2, a and d).

### *Voltammetric studies*

The  $\text{BaPb}_{0.9}\text{Sb}_{0.1}\text{O}_3$  pellets were used as anodes in voltammetric studies performed in sodium sulphate aqueous solutions with and without guaiacol. Fig. 3 shows representative curves for both systems. It can be seen that, in the absence of guaiacol the system presents electrochemical stability for a wide

range of potentials, between 0 and 1.5 V vs. Ag/AgCl, KCl sat. Just before oxygen evolution, a shoulder appears, which was assigned to the oxidation of the sulphate to the persulphate, in solution, on the basis of the calculated equilibrium potential for this process at pH=7 (1.724 V vs. Ag/AgCl) [28]. In the presence of 100 mg L<sup>-1</sup> guaiacol, the voltammetric pattern is similar between -0.5 V and 1.5 V. However, near the electrolyte oxidation it can be seen an increase in the anodic peak current intensity that can be due to a simultaneous guaiacol oxidation. When a higher guaiacol concentration was used (1000 mg L<sup>-1</sup>), an extra anodic peak near 0.5 V appears due to the guaiacol oxidation with polymerisation, which consequently decreases the second peak intensity due to a partial passivation of the electrode's surface. The guaiacol oxidation can occur before oxygen evolution but with low efficiency, due to electrode's passivation. So, in the degradation assays high current densities were applied (5 and 10 mA cm<sup>-2</sup>) to guarantee oxygen evolution, thus avoiding electrodes' passivation.

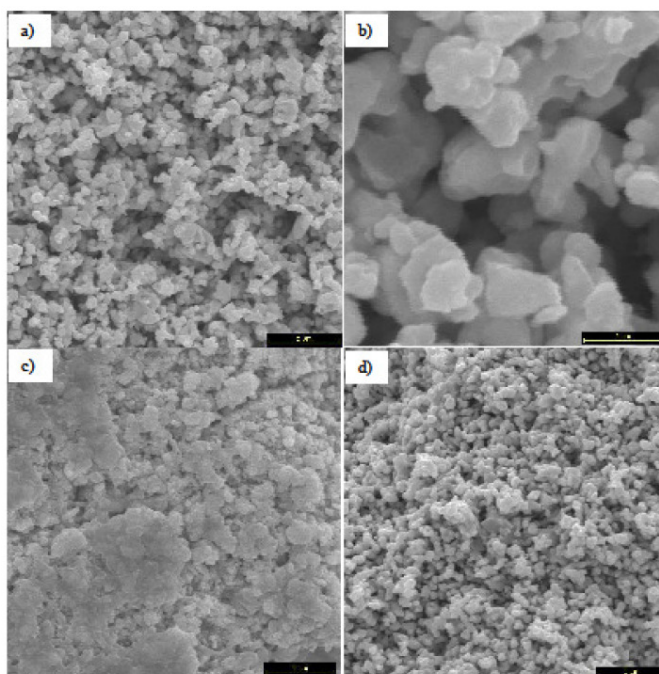
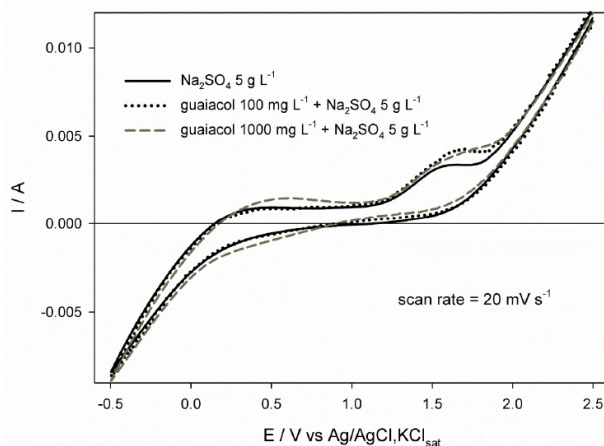


**Figure 2.** SEM micrographs of BaPb<sub>0.9</sub>Sb<sub>0.1</sub>O<sub>3</sub> electrodes, before being used, with magnifications of a) 2500x and b) 10000x, and after being used, with a magnification of 2500x, c) outer layer of the electrode and d) electrode cross-section.

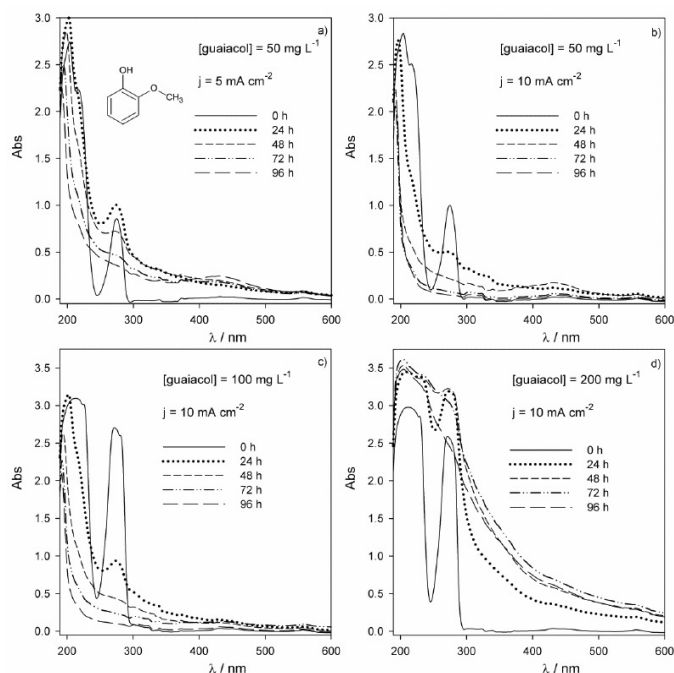
### ***Electrodegradation assays***

Fig. 4 presents the UV-Vis spectra for the samples collected at different reaction times in the electrodegradation assays performed at different experimental conditions. The spectrum of the initial solution presents a band, in the UV region, at 276 nm, characteristic of the aromatic compounds. Depending on the ratio guaiacol concentration/applied current density there is an increase or a decrease of the absorbance of the solution at this wavelength. The increase in absorbance was not expected, since there is always a gradual guaiacol degradation in time, as observed by COD and DOC simultaneous decays (Fig. 5, a to d). It is due to the formation of products with very low solubility that promote the turbidity of the solutions. This effect is more pronounced when the ratio guaiacol

concentration/applied current density is higher, because there are less electrons available for guaiacol complete oxidation and the dimmers resulting from the one-electron guaiacol oxidation are formed with higher concentration [15]. The evidence of these dimmers formation is the increase, in the first part of the assays, of the absorbance measured at 470 nm, followed by a decrease, when the guaiacol concentration decreases.



**Figure 3.** Cyclic voltammograms for  $\text{BaPb}_{0.9}\text{Sb}_{0.1}\text{O}_3 / \text{Na}_2\text{SO}_4$  ( $5 \text{ g L}^{-1}$ ) and  $\text{BaPb}_{0.9}\text{Sb}_{0.1}\text{O}_3 / \text{Na}_2\text{SO}_4$  ( $5 \text{ g L}^{-1}$ ) + guaiacol ( $100$  and  $1000 \text{ g L}^{-1}$ ) systems. Scan rate  $20 \text{ mV s}^{-1}$ ; working electrode geometric area  $1.3 \text{ cm}^2$ .



**Figure 4.** UV-Visible spectra for the samples collected at different reaction times for guaiacol electrochemical degradation assays performed with different current densities and guaiacol initial concentrations. Inset of a): Guaiacol chemical structure.

The relative COD and DOC decays for the different experimental conditions assayed (Fig. 5) show a regular removal of the organic load from the solutions. There is an increase in COD and DOC decays with the increase in current

density, for equal initial guaiacol concentration (Fig. 5, a and b). There is also an increase in that parameters decay with concentration, for the assays performed with 5 mA cm<sup>-2</sup> (Fig. 5, c). The influence of the concentration at 10 mA cm<sup>-2</sup> applied current density is not clear in Fig. 5d. However, from the data presented in Table 1, of the absolute removals of COD and DOC at different experimental conditions, after 120 hours run, it can be inferred that an increase in the initial concentration also led to an increase in COD and DOC removals.

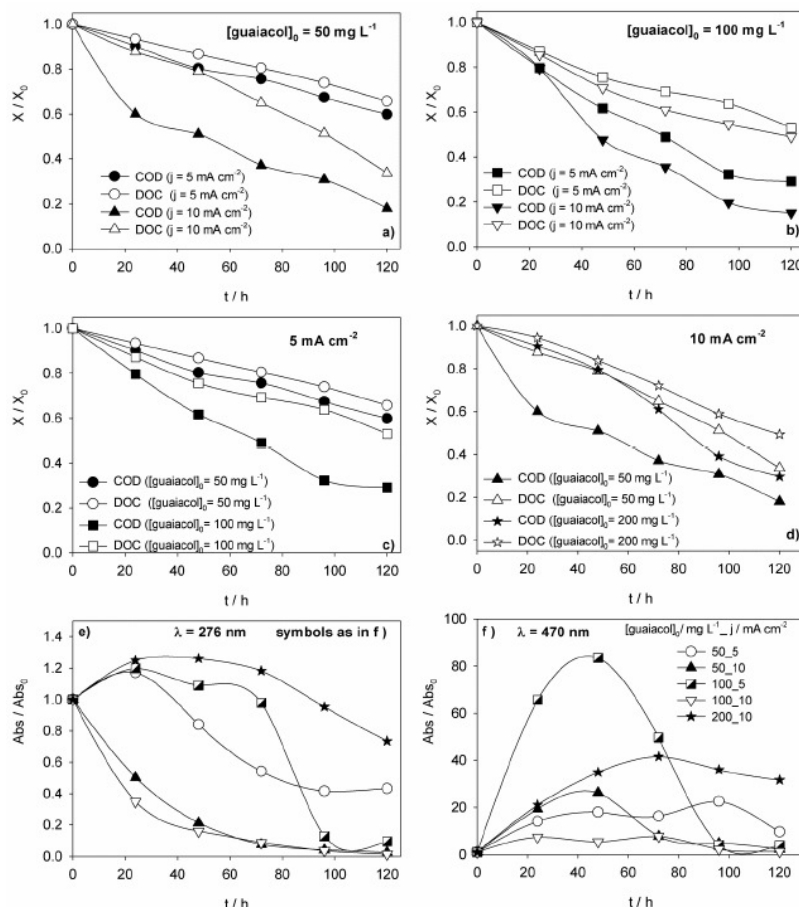


**Figure 5.** Relative decays of COD and DOC (a to d) and absorbances, measured at (e) 276 and (f) 470 nm, for the guaiacol electrodegradation assays performed with different experimental conditions.

**Table 1.** Removal of COD and DOC, after 120 h assay, and combustion efficiency for the different experimental conditions tested.

Current density / mA cm <sup>-2</sup>	[Guaiacol] <sub>0</sub> / mg L <sup>-1</sup>	ΔCOD <sub>0 h-120 h</sub> / mg L <sup>-1</sup>	COD % removal	ΔDOC <sub>0 h-120 h</sub> / mg L <sup>-1</sup>	DOC % removal	η <sub>c</sub>
5	50	58±5	40	12.2±0.9	34	0.65
	100	176±12	71	37.0±0.5	47	0.61
10	50	117±7	82	27±2	66	0.45
	100	211±8	85	44±2	51	0.60
	200	270±9	70	69±3	51	0.76

The analysis of the results regarding the controlling step of the degradation is not straightforward. If the process was diffusion controlled, COD removals should be

independent of the applied current density. On the other hand, if the process had a kinetic control, an increase in concentration would not lead to an increase in COD removal. Thus, the behaviour presented by the system in response to any increase in guaiacol concentration or in current density is typical from processes where the indirect oxidation is an important factor. In fact, all the assays were performed at current densities where oxygen evolution is occurring, since  $5 \text{ mA cm}^{-2}$  corresponds to a current intensity of 6.5 mA (see Fig. 3), thus allowing the formation of hydroxyl radicals. The chemical reactivity of the hydroxyl radicals is strongly connected with their interaction with the metal oxide ( $\text{MO}_x$ ) surface. Oxides in which the oxidation state of the metals are the highest possible, the interaction of the radicals with the surface of the oxide is weaker (non-active electrodes) making them more reactive and encouraging mineralization. On the contrary, if the metals are not in the maximum oxidation state (active electrode), the chemical bond formed between the radical and the metal oxide active sites leads to the formation of the intermediate  $\text{MO}_{x+1}$ , less reactive towards the pollutant [29]. In the case of  $\text{BaPb}_{0.9}\text{Sb}_{0.1}\text{O}_3$ , although there is evidence that Pb and Sb are mainly in the highest oxidation states [11] (non-active anode), some active sites may not be completely oxidized [30], leading to the formation of the less reactive intermediate  $\text{MO}_{x+1}$  and to the conversion of the organic pollutants over their mineralization. Moreover, taking into account the CV analysis, the role in the guaiacol oxidation by the persulphate ion, formed by sulphate oxidation, cannot be excluded.

The relative variation of the absorbance measured at 276 and 470 nm is presented in Fig. 5, e and f, respectively. The turbidity of the solution, related with the formation of dimmers, increases for high initial concentration/current density ratios.

To evaluate the influence of the experimental conditions on the extension of the guaiacol mineralization, the combustion efficiency,  $\eta_c$ , which relates the removal of carbon from the solution (mineralization) with the oxidation state of the organic compounds in solution (conversion), was calculated according to the model developed by Pacheco et al. [16]:

$$\eta_c = \frac{32}{12} \left( \frac{n}{4x} \right) \frac{\Delta\text{DOC}}{\Delta\text{COD}} \quad (1)$$

where DOC is in  $\text{mg L}^{-1}$ , COD is in  $\text{mg L}^{-1}$ ,  $n$  is the number of electrons transferred to the electrode in the complete combustion of the organic pollutant molecule (eq. 2),  $x$  is the number of carbon atoms in the organic compound and  $\frac{\Delta\text{DOC}}{\Delta\text{COD}}$  is the slope of the DOC vs. COD plot.



The DOC vs. COD plots are presented in Fig. 6 and, substituting these slopes on eq. 1, the combustion efficiency for the different assays can be determined. Results are presented in Table 1, showing that high initial concentration/current density ratios promote combustion, whereas low initial concentration/current density ratios promote conversion. This last conclusion is evident in Fig. 6, where for an initial guaiacol concentration of  $50 \text{ mg L}^{-1}$  and a current density of

10 mA cm<sup>-2</sup> the DOC vs. COD plot only presents a linear regression for the first part of the assay, pointing towards the existence of different products in the second part of the assay.

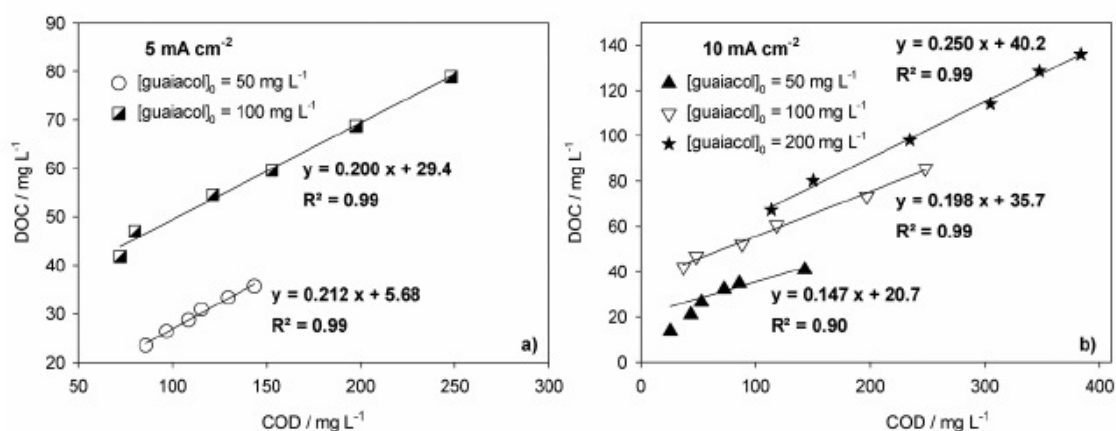


**Figure 6.** Variation of DOC with COD for the different initial concentrations tested at a) 5 and b) 10 mA cm<sup>-2</sup> applied current density. Lines represent the adjusted linear equations, whose slopes are used in eq. 1 to calculate the combustion efficiency.

## Conclusions

BaPb<sub>0.9</sub>Sb<sub>0.1</sub>O<sub>3</sub> perovskite oxides prepared by ceramic route presented an X-ray diffraction pattern similar to the perovskite BaPbO<sub>3</sub>, indicating the presence of a single phase material.

The electrodegradation of guaiacol using BaPb<sub>0.9</sub>Sb<sub>0.1</sub>O<sub>3</sub> as anode material was performed with good organic load removal, being the highest absolute COD and DOC removals obtained for the assays performed at the highest current density and initial guaiacol concentration. This perovskite has shown very good mechanical stability, even at the applied current density of 10 mA cm<sup>-2</sup>, since no breakdown of the electrode crystallites was observed.

Combustion efficiencies between 0.45 and 0.76 were attained, being the highest value obtained for an initial guaiacol concentration of 200 mg L<sup>-1</sup> and an applied current density of 10 mA cm<sup>-2</sup>.

## Acknowledgements

Financial support from Fundação para a Ciência e a Tecnologia, FCT, for the project PEst-OE/CTM/UI0195/2011 and for the grant awarded to A. Rodrigues, is gratefully acknowledged.

## References

1. Bockris JO'M, Otagawa T. J Electrochem Soc. 1984;131:290-302.
2. Balej J. Int J Hydrog Energy. 1985;10:89-99.
3. Amado RS, Malta LFB, Garrido FMS, et al. Quim Nova. 2007;30:189-197.
4. Yu T, Mao X, Ma G. J Alloy Comp. 2014;608:30-34.

5. Krishtalik LI. *Electrochim Acta*. 1981;26:329-337.
6. Ciríaco MLF, Pereira MIS, Nunes MR, et al. *Port Electrochim Acta*. 1999;17:149.
7. Ciríaco MLF, Pereira MIS, Nunes MR, et al. *J Solid State Electrochem*. 2001;5:495.
8. Pacheco MJ, Ciríaco MLF, Lopes A, et al. *Port Electrochim Acta*. 2006;24:273-282.
9. Zhang L, Nie Y, Hu C, et al. *Appl Catal B-Environ*. 2012;125:418- 424.
10. Pacheco MJ, Regalado F, Santos D, et al. *J Electrochem Soc*. 2014;161:H474-H480.
11. Eibschütz M, Reiff WM, Cava RJ, et al. *Appl Phys Lett*. 1990;56:2339-2341.
12. Yasukawa M, Kadota A, Maruta M, et al. *Solid State Commun*. 2002;124:49-52.
13. Paula M, Van S, Young LY. *Appl Environ Microbiol*. 1998;64:2432-2438.
14. Sharma N, Gupta VC. *Int J Chem Eng Appl*. 2012;3:182-186.
15. Doerge DR, Divi RL, Churchwell MI. *Anal Biochem*. 1997;250:10-17.
16. Pacheco MJ, Morão A, Lopes A, et al. *Electrochim Acta*. 2007;53:629-636.
17. Samet Y, Elaoud SC, Ammar S, et al. *J Hazard Mat. B*. 2006;138:614-619.
18. Panizza M, Cerisola G. *Electrochim Acta*. 2005;51:191-199.
19. Panizza M, Cerisola G. *Water Res*. 2009;43:339-344.
20. Comninellis Ch, Pulgarin C. *J Appl Electrochem*. 1991;21:703-708.
21. Comninellis Ch, Pulgarin C. *J Appl Electrochem*. 1993;23:108-112.
22. Pannizza M, Michaud P-A, Cerisola G, et al. *Electrochem Commun*. 2001;3:336-339.
23. Iniesta J, Michaud PA, Panizza M, et al. *Electrochim Acta*. 2001;46:3573-3578.
24. Morão A, Lopes A, Pessoa de Amorim MT, et al. *Electrochim Acta*. 2004;49:1587- 1595.
25. Cañizares P, Lobato J, Paz R, et al. *Water Res*. 2005;39:2687-2703.
26. Eaton A, Clesceri L, Greenberg A. *Standard methods for examination of water and wastewater*. 19 th Edition. 1995.
27. Holland TJB, Redfern SAT. Unicell, computer program developed at the University of Cambridge. 1995.
28. Pourbaix M. *Atlas d'équilibres électrochimiques à 25 °C*. 1<sup>ere</sup> Ed. Paris:Gauthier-Villars & C<sup>ie</sup> Éditeur; 1963.
29. Simond O, Schaller V, Comninellis C. *Electrochim Acta*. 1997;42:2009-2012.
30. Cava RJ, Batlogg B, Espinosa GP, et al. *Nature*. 1989;339:291-293.